THE JOURNAL OF BIOLOGICAL CHEMISTRY VOL. 281, NO. 39, pp. 28666–28678, September 29, 2006
© 2006 by The American Society for Biochemistry and Molecular Biology, Inc. Printed in the U.S.A.

Regulation of Mouse Inducible Costimulator (ICOS) Expression by Fyn-NFATc2 and ERK Signaling in T Cells*

Received for publication, April 28, 2006, and in revised form, July 31, 2006 Published, JBC Papers in Press, July 31, 2006, DOI 10.1074/jbc.M604081200

Andy Hee-Meng Tan[1], **Siew-Cheng Wong**[1], **and Kong-Peng Lam**[2]

From the Laboratory of Immune Regulation, Singapore Institute of Immunology, Proteos, Singapore 138673, Singapore

The inducible costimulator (ICOS), a member of the CD28 family of costimulatory molecules, is rapidly induced upon T cell activation. Although the critical role of ICOS in costimulating T cell responses is well documented, little is known of the intracellular signaling pathways and mechanisms that regulate ICOS expression. Here, we report that Fyn, NFAT, and ERK signaling influence ICOS expression as various chemical inhibitors, such as PP2 that targets Src kinases, U0126 that targets MEK1/2, and cyclosporin A or FK506 that targets calcineurin and thereby affects NFAT, attenuate T cell receptor-mediated ICOS induction. Moreover, ectopic expression of NFATc2 or a constitutively active MEK2 amplifies ICOS transcription and transactivates a 288-bp core region of the *icos* promoter in luciferase reporter assays. We also identify a site on the *icos* promoter that is sensitive to ERK signaling and further show that NFATc2 can bind the *icos* promoter *in vivo* and that this binding is diminished when Fyn signaling is ablated. The normal activation of ERK but reduced nuclear translocation of NFATc2 in Fyn$^{-/-}$ CD4^{+} T cells further suggest that Fyn and NFATc2 act in a common axis, separate from that involving ERK, to drive ICOS transcription. Taken together, our findings indicate that Fyn-calcineurin-NFATc2 and MEK2-ERK1/2 are two independent signaling pathways that cooperate to control T cell receptor-mediated ICOS induction.

T lymphocytes require two signals to be fully activated. The first, an antigen-specific signal, is delivered via the T cell receptor (TCR),[3] whereas the second, a costimulation signal, is sent mainly via a member of the CD28 family of molecules found on the surface of T cells (1, 2). The costimulation signal is critical in maintaining the full activation status of antigen-stimulated T cells by sustaining their cellular proliferation and differentiation, thus preventing onset of anergy and induction of apoptosis.

The CD28 family of molecules are type I transmembrane glycoproteins and possess putative Src homology 2 and 3 motifs in their cytoplasmic tails for signal transduction. The prototypic member, CD28, is expressed constitutively on naive T cells and engaged by the B7-1 (CD80) and B7-2 (CD86) molecules on antigen-presenting cells, such as macrophages, B cells, and dendritic cells. Cognate interaction between CD28 and B7-1 and B7-2 ligands will lead to IL-2 transcription (3), expression of CD25 (IL-2Rα), and entry into cell cycle as well as induced expression of the cell survival protein Bcl-X_L in T cells (4). Another CD28 family member, CTLA-4, acts as a negative regulator in this co-stimulatory pathway by competing for binding to the same B7 ligands and thereby inhibiting IL-2 synthesis and cell cycle progression and thus terminating T cell responses (2).

Although CD28 is the predominant costimulatory molecule, it does not account for all costimulatory functions in T cells. Mice lacking CD28 are still able to mount effective responses to some viruses (5). Furthermore, the production of effector cytokines such as inteferon-γ and IL-4 can still be stimulated to normal levels by antigen-presenting cells lacking B7 ligands (6). In contrast to naive T cells, the reactivation of antigen-experienced T cells also appears to be less dependent on CD28/B7 interaction (7, 8). These results suggest that other costimulatory molecules can compensate for the lack of CD28 signaling. One candidate is the recently discovered inducible costimulator (ICOS), which is also a member of the CD28 family of receptors.

ICOS shares 30–40% sequence similarity to CD28 and CTLA-4 but does not have the conserved extracellular MYPPPY motif necessary for binding B7-1 and B7-2 (9, 10). Instead, it binds a different cell surface molecule known as ICOS ligand (ICOSL, also termed B7h, B7RP-1, GL-50, LICOS, or B7-H2) that is expressed constitutively on B cells and at low levels on monocytes and whose expression can be induced in fibroblasts, nonlymphoid tissues, and other nonprofessional antigen-presenting cells (11, 12). ICOS is expressed in both CD4^{+} and CD8^{+} T cells and may play a more important role in costimulating effector and memory T cells as compared with naive T cells (13). ICOS engagement *in vitro* can contribute to the production of cytokines, such as IFN-γ, tumor necrosis factor-α, IL-4, IL-5, and IL-10, but little IL-2 (9, 12, 14). Recent studies also indicate that in the absence of CD28, ICOS appears to assume the major T cell costimulatory role for humoral immune responses (15).

* This work was supported by grants from the Biomedical Research Council of the Agency for Science, Technology and Research, Singapore. The costs of publication of this article were defrayed in part by the payment of page charges. This article must therefore be hereby marked "*advertisement*" in accordance with 18 U.S.C. Section 1734 solely to indicate this fact.

[1] These authors contributed equally to this work.

[2] To whom correspondence should be addressed: Laboratory of Immune Regulation, Singapore Institute of Immunology, 61 Biopolis Dr., Proteos, Singapore 138673, Singapore. Tel.: 65-65869649; Fax: 65-67791117; E-mail: mcblamkp@imcb.a-star.edu.sg.

[3] The abbreviations used are: TCR, T cell receptor; NFAT, nuclear factor of activated T cells; ERK, extracellular signal-regulated kinase; CsA, cyclosporin A; TSS, transcriptional start site; Luc, luciferase; PMA, phorbol-12-myristate-13-acetate; TF, transcription factor; EMSA, electrophoretic mobility shift assay; ChIP, chromatin immunoprecipitation; IL, interleukin; GC, germinal center; MEK, mitogen-activated protein kinase/extracellular signal-regulated kinase kinase; RT, reverse transcription; RLU, relative light units; Ab, antibody; P/I, PMA and ionomycin; caMEK2, constitutively active form of MEK2; PP2, Src kinase inhibitor; JNK, c-Jun NH_2-terminal kinase.

This is an Open Access article under the CC BY license.

Characterization of ICOS-deficient mice revealed that the absence of ICOS impaired humoral immune responses by affecting germinal center (GC) formation and B cell immunoglobulin class switching (16–19). Consistent with a pivotal role for ICOS in GC development, ICOS has been implicated in the maintenance of $CXCR5^+$ follicular B helper T cells *in vivo* (20). Human ICOS deficiency, on the other hand, results in a clinical phenotype indistinguishable from that of adult onset common variable immunodeficiency (21, 22). The importance of ICOS/ICOSL in costimulating immune reactions can be glimpsed from various murine disease models. In the examples of experimental autoimmune encephalomyelitis and cardiac allograft transplantation, ICOS blockade could abrogate immunopathogenesis or prolong allograft survival, respectively (23, 24). Moreover, interference of the ICOS-ICOSL pathway has also been shown to result in the resolution of mercury-induced autoimmunity (25). Last, but not least, ICOS/ICOSL interactions have also been implicated in Th2-mediated allergic diseases, such as airway hypersensitivity (26), allergy and asthma (27), and acute or chronic graft *versus* host disease (28).

Despite extensive studies pointing to a crucial role for ICOS in cellular and humoral immunity, little is known about the regulation of ICOS expression. ICOS is absent or expressed at low levels on naive T cells and is rapidly up-regulated upon T cell activation (19, 29). It is envisaged that the ability to enhance ICOS expression at the appropriate time could lead to more effective immune responses against pathogens. Conversely, the ability to down-regulate ICOS expression could modulate the rejection of organ and tissue transplantation and alleviate the severity of autoimmune diseases. Hence, in the present study, we elucidated the signaling pathways originating from TCR and CD28 costimulation that lead to ICOS induction as well as delineate the *cis*-acting regulatory region and *trans*-acting transcription factors (TFs) that govern ICOS transcription. We found that the Fyn-calcineurin-NFATc2 and MEK2-ERK1/2 signaling pathways operate independently but converge on the *icos* core promoter to induce ICOS transcription.

EXPERIMENTAL PROCEDURES

Mouse Strains, Cell Lines, Antibodies, and Chemical Inhibitors—Wild-type C57BL/6 mice were obtained from the Singapore Biological Resource Centre. B6.129S7-*Fyn*^{tm1Sor}/J ($Fyn^{-/-}$) mice were purchased from Jackson Laboratory. All mice were bred and used between 8 and 12 weeks of age according to institutional guidelines. The murine EL4 thymoma cell line was maintained in complete RPMI 1640 medium supplemented with 10% fetal calf serum (HyClone, Logan, UT), 2 mM L-glutamine, 50 mg/ml penicillin, 50 mg/ml streptomycin, 100 mM HEPES, and 55 μM β-mercaptoethanol. Anti-CD3 (145-2C11) and anti-CD28 (37.51) antibodies for cell stimulation, fluorescein isothiocyanate-conjugated anti-CD4 (GK1.5), anti-CD8 (53-6.7), and biotin-conjugated anti-ICOS (7E.17G9) antibodies and PE-Cy5-conjugated streptavidin for flow cytometric staining were obtained from BD Biosciences. Chemical inhibitors FK506 (10 μM), CsA (low dose, 5 ng/ml; high dose, 50 ng/ml), wortmannin (100 nM), and rapamycin (10 nM) were obtained from Sigma. PP2 (5 μM), damnacanthal (100 nM), piceatannol (50 μM), SB203580 (10 μM), JNK inhibitor I (5 μM), and NF-κB competitor peptide SN50 (10 μM) were purchased from Calbiochem. U0126 (50 μM) was obtained from Cell Signaling Technology (Beverly, MA).

$CD4^+$ T Cell Purification, Activation, and Flow Cytometric Analyses—Single cell suspensions were prepared from lymph nodes and spleens of $Fyn^{+/+}$ and $Fyn^{-/-}$ mice and treated with red blood cell lysing solution (0.15 M NH_4Cl and 0.1 mM Na_2EDTA) for 5 min at 4 °C to eliminate erythrocytes. $CD4^+$ T cells were positively isolated using anti-CD4 antibody (monoclonal antibody)-coupled magnetic cell-sorting microbeads (Miltenyi Biotech, Bergisch Gladbach, Germany) to more than 95% purity (as analyzed by flow cytometric staining with anti-CD4 and anti-CD8 antibodies). Purified $CD4^+$ T cells (5×10^5) were either untreated or seeded into 24-well tissue culture plates precoated with 1 μg/ml anti-CD3 and 4 μg/ml soluble anti-CD28 monoclonal antibodies. In some experiments, $CD4^+$ T cells were incubated with chemical inhibitors 1 h prior to activation. Cells were stained with fluorochrome-conjugated anti-CD4 and anti-ICOS antibodies and analyzed on a FACScan using CellQuest software (BD Biosciences).

RNA Isolation and Real Time RT-PCR Analyses—Total RNA was isolated using TRIzol and treated with DNase I (Invitrogen) to avoid DNA contamination; cDNA was prepared using SuperScript III reverse transcriptase (Invitrogen) with oligo$(dT)_{12-18}$ as primer. Primers used for real time PCR were as follows: ICOS, 5′-TGA CCC ACC TCC TTT TCA AG-3′ and 5′-TTA GGG TCA TGC ACA CTG GA-3′; β-actin, 5′-GAT CTG GCA CCA CAC CTT CT-3′ and 5′-ACC AGA GGC ATA CAG GGA CA-3′. Each reaction (95 °C, 2 min; 95 °C, 10 s; 60 °C, 30 s; 72 °C, 30 s, 40 cycles) was performed using QuantiTect SYBR Green PCR kit (Qiagen, Valencia, CA) in a Mx3000P QPCR System (Stratagene). All experiments were repeated twice, mRNA levels of ICOS were normalized against β-actin, and mRNA levels in treated cells were expressed as -fold change relative to those in untreated cells. Statistical analysis (unpaired two-tailed Student's *t* test) was performed with PRISM software (GraphPad Software, San Diego, CA).

Immunoprecipitation and Western Blotting—Cells ($2–5 \times 10^6$) were lysed on ice for 15 min in buffer containing 1% (v/v) Nonidet P-40, 10 mM Tris-HCl (pH 8.0), 150 mM NaCl, 1 mM EDTA, 0.2 mM Na_3VO_4, 1 mM phenylmethylsulfonyl fluoride, and 10 μg/ml aprotinin, and cell debris was removed by centrifugation at 13,000 rpm for 12 min at 4 °C. For immunoprecipitation, cell lysates were sequentially incubated with 2–2.5 μg of appropriate antibodies and protein A/G PLUS-agarose beads (Santa Cruz Biotechnology, Inc., Santa Cruz, CA). Following determination of protein concentrations using a Bradford assay (Bio-Rad), the samples were loaded in appropriate amounts and electrophoresed in a 7–10% SDS-PAGE, electroblotted onto polyvinylidene difluoride membrane, and probed with Abs that recognize specific proteins. Protein bands were visualized using horseradish peroxidase-coupled Abs and an enhanced chemiluminescence detection system (SuperSignal West Pico Chemiluminescent Substrate System; Pierce). Antibodies against phospho-ERK (E-4), ERK2 (C-14), NFATc2 (G1-D10), and TFIID (58C9) were obtained from Santa Cruz Biotechnology.

Plasmid Constructs, Transient Transfections, and Luciferase Reporter Assays—The *icos* promoter, spanning −1478 to −1 relative to the first nucleotide of the mouse cDNA (NCBI GenBank™ accession number NM_017480) was amplified from C57BL/6 mouse genomic DNA by PCR using primers carrying restriction sites for KpnI and HindIII (5′-GAG CAG TCA TTG AGA GGC CAG AAG AG-3′ and 5′-CCC AAG CTT AGT GCT CAA AAG TGT CAG-3′) and cloned into the promoterless luciferase plasmid vector, pGL3-Basic (pGL3B; Promega, Madison, WI) to create mICOSp(−1478)-Luc. 5′ deletion mutants of this promoter fragment were either generated after suitable restriction enzyme digestion and religated into pGL3B or subcloned by nested PCR to create mICOSp(−900)-Luc, mICOSp(−599)-Luc, mICOSp(−471)-Luc, mICOSp(−288)-Luc, mICOSp(−147)-Luc, mICOSp(−109)-Luc, and mICOSp(−52)-Luc. A 3-bp region, CTT, between bp 142 and 144 within mICOSp(−288)-Luc was replaced by AGA using the QuikChange site-directed mutagenesis kit (Stratagene) to create mICOSp(−288)-ERK-mut-Luc. The same protocol was used to replace a 2-bp section, CC, between bp 231 and 232 with AA in mICOS(−288)-Luc to generate mICOSp(−288)-NFAT-mut-Luc. 0.98 μg of the luciferase reporter plasmid and 0.02 μg of pRL-TK (*Renilla*) plasmid (50:1 ratio) were premixed in OPTI-MEM I reduced serum medium (Invitrogen) and transiently transfected with Lipofectamine 2000 (Invitrogen) in triplicate into EL4 cells seeded in 24-well flat bottom plates at 1×10^6 cells/ml in 0.5 ml of RPMI 1640 medium without antibiotics. Cells were incubated at 37 °C in 5% CO_2 for 4 h before stimulation with 10 ng/ml PMA and 0.5 μg/ml ionomycin. Cells were cultured for another 14–16 h and harvested by centrifugation. Cell pellets were solubilized in passive lysis buffer (Promega) and incubated on a Spiramix roller mixer for 15 min at room temperature. 20 μl of cell lysate was assayed for both firefly and *Renilla* luciferase activities using the dual luciferase reporter assay system (Promega), and relative light units (RLU) were measured in a TD-20/20 single tube luminometer (Turner BioSystems, Sunnyvale, CA). RLU from the firefly luciferase was normalized for transfection efficiency to the *Renilla* luciferase RLU in each lysate (normalized RLU = $RLU_{\text{firefly luciferase}}/RLU_{\textit{Renilla}\text{ luciferase}}$). For *icos* promoter analysis, the activity of a reporter construct following stimulation was calculated as follows: reporter activity = normalized $RLU_{\text{stimulated}}$/normalized $RLU_{\text{unstimulated}}$. For the effect of overexpressed proteins on *icos* promoter activity, the -fold induction was calculated as follows: -Fold induction = normalized $RLU_{\text{protein-expressing vector, unstimulated or stimulated}}$/normalized $RLU_{\text{null vector, unstimulated}}$. The pUSEamp vector expressing a constitutively active form of MEK2 (S222D/S226D double mutant) was purchased from Upstate Biotechnology, Inc. (Lake Placid, NY). The pBJ5 and pBJ5-NFATc1 vectors were generously provided by Dr. Neil A. Clipstone (Northwestern University, Chicago, IL). The pBJ5-NFATc2 (pSH210) and pBJ5-NFATc3 (pSH250A) vectors were kind gifts from Dr. Gerald R. Crabtree (Stanford University, Stanford, CA). Sequences of all DNA constructs were confirmed by automated sequence analyses.

Chromatin Immunoprecipitation (ChIP)—ChIP was performed according to the manufacturer's protocol (Upstate Biotechnology). Briefly, cells (2×10^6) were treated with anti-CD3 and anti-CD28 monoclonal antibodies for 16 h, cross-linked with 1% formaldehyde for 10 min at 37 °C, washed with ice-cold phosphate-buffered saline containing 1 mM phenylmethylsulfonyl fluoride, harvested, and lysed in SDS buffer. DNA was sheared by ultrasonication using a high intensity ultrasonic processor (Heat Systems) for 8 × 12-s pulses at 30% amplitude. Lysates were centrifuged, resuspended in ChIP dilution buffer, and precleared using salmon sperm DNA/protein A-agarose. Protein-DNA complexes were immunoprecipitated with 6 μg of anti-NFATc2 or isotype-matched control Ab (mouse IgG2a) overnight at 4 °C. Ab-protein-DNA complexes were then captured using salmon sperm DNA-protein A-agarose for 1 h at 4 °C. After washing beads with low and high salt LiCl and TE buffers, the protein-DNA complexes were eluted using 1% SDS, 0.1 M $NaHCO_3$ buffer and disrupted by heating at 65 °C for 4 h. DNA was then phenol/chloroform-extracted and ethanol-precipitated and subjected to PCR using primers spanning −288 to transcription start site (TSS) of the *icos* promoter: sense, 5′-CCG CTC GAG CAT GCA TGC ATC CAT C-3′; antisense, 5′-CCC AAG CTT AGT GCT CAA AAG TGT CAG-3′ (94 °C, 15 s; 60 °C, 30 s; 72 °C, 1 min, 28 cycles). PCR products were then separated on 2% agarose gels.

Electrophoretic Mobility Shift Assay (EMSA)—Nuclear extracts were prepared using the NE-PER nuclear and cytoplasmic extraction reagents kit (Pierce). Briefly, cells (10×10^6) were untreated or stimulated for 16 h and washed in phosphate-buffered saline at 4 °C. Nuclear extracts were prepared by hypotonic lysis and high salt extraction and subsequently cleared of insoluble material by centrifugation at 13,000 rpm for 5 min at 4 °C before being concentrated with a Microcon-3 column (Millipore Corp., Billerica, MA). Nuclear extracts were stored at −80 °C prior to use, and protein content was measured using a Bradford assay (Bio-Rad). For gel shift assays, double-stranded oligonucleotide probes were end-labeled with [γ-^{32}P]ATP using T4 polynucleotide kinase (New England Biolabs, Beverly, MA). Labeled probes were purified using ProbeQuant G-50 microcolumns (Amersham Biosciences). Binding reactions were conducted at room temperature for 20 min in a 20-μl total volume containing 0.5 ng of labeled probe, 5 μg of nuclear extract, 1 μg of poly(dI·dC) (Amersham Biosciences), and gel shift buffer (12 mM HEPES, pH 7.9, 4 mM Tris-HCl, pH 7.9, 60 mM KCl, 5 mM $MgCl_2$, 5 mM dithiothreitol, and 12.5% glycerol). For competition assays, competing oligonucleotides were preincubated with the reaction mix at room temperature for 15 min before the addition of radiolabeled probe. Binding reactions were size-fractionated using a 5% nondenaturing PAGE in 0.5× TBE and electrophoresed at 120 V for 4 h at room temperature. The gel was subsequently transferred onto 3MM chromatography paper, dried, and exposed to autoradiographic film for 1 to 3 days at −80 °C. The probe sequences were as follows: p154_105, 5′-TCA CCG GGT ACT TGC CAT GCA GGA GGC GCT GTG ATA GCT CTC CAA GTA GA-3′; p154_130, 5′-TCA CCG GGT ACT TGC CAT GCA GGA G-3′. Competitor sequences were p154_105, as above; p154_130, as above; p129_105, 5′-GCG CTG TGA TAG CTC TCC AAG TAG A-3′;

p154_130_mut, 5′-TCA CCG GGT AAG A[4]GC CAT GCA GGA G-3′; NF-κB consensus, 5′-AGT TGA GGG GAC TTT CCC AGG C-3′; NFATc consensus, 5′-CGC CCA AAG AGG AAA ATT TGT TTC ATA-3′; Ets-1 consensus, 5′-GAT CTC GAG CAG GAA GTT CGA-3′; Elk-1 consensus, 5′-GGG CTG CTT GAG GAA GTA TAA GAA T-3′; Elf-1, 5′-CTT GGG GGC AGG ACT TCC TGT TTC T-3′ (30); CP2/LSF consensus, 5′-GTC TGA TTT CAC AGG AA-3′ (31); Sp1 consensus, 5′-ATT CGA TCG GGG CGG GGC GAG C-3′; AP1 consensus, 5′-CGC TTG ATG ACT CAG CCG GAA-3′.

RESULTS

ICOS Induction by TCR and CD28 Co-engagement Is Subject to Transcriptional Control—ICOS expression is induced upon T cell activation and, in particular, in response to TCR and CD28 co-engagement (29). To examine in detail the kinetics of ICOS induction, we first determined the level of ICOS cell surface expression and correlated that with the induction of ICOS mRNA in murine primary $CD4^+$ T cells stimulated with anti-CD3 and anti-CD28 antibodies, which engaged the TCR and CD28, respectively (henceforth designated as TCR/CD28). As shown in Fig. 1*A*, an increase in cell surface expression of ICOS could be detected as early as at 6 h of T cell activation using a fluorochrome-conjugated anti-ICOS antibody in flow cytometry analysis, and the expression level seems to peak at 40 h of T cell stimulation. At the transcriptional level, an increase in ICOS mRNA could be detected via real time RT-PCR as early as 3 h after TCR/CD28 stimulation, and the mRNA level appeared to peak and plateau from 6 to 18 h before declining (Fig. 1*B*). Thus, it was evident from the temporal increase in mRNA and cell surface protein expression that ICOS was subjected to some level of transcriptional control.

ICOS Expression Is Regulated by Distinct Pathways Downstream of TCR and CD28 Signaling—Since TCR/CD28 stimulation could lead to an increase in ICOS mRNA and cell surface protein expression, we were interested to characterize the signaling pathways that regulate ICOS induction. To accomplish this, we first utilized a range of chemical inhibitors to block intracellular signaling pathways known to be activated by TCR/CD28 engagement in primary $CD4^+$ T cells and assessed their effects on cell surface ICOS induction (Fig. 2*A*). Our data show that FK506 (tacrolimus), which is known to inhibit calcineurin, substantially diminished cell surface expression of ICOS on activated T cells, thus suggesting a possible role for this pathway in ICOS induction. This was consistent with a previous study that showed an inhibitory effect of CsA, which also deactivates calcineurin, on ICOS induction in human $CD4^+$ T cells (9). Furthermore, since calcineurin is Ca^{2+}-sensitive, blocking Ca^{2+} elevation in general (*e.g.* with EGTA) also mitigated the induction of ICOS (data not shown). To determine whether the reduction in cell surface expression of ICOS on activated T cells by FK506 treatment was in part a consequence of transcriptional reduction, we assayed for the amount of ICOS mRNA in FK506- and CsA-treated TCR/CD28-stimulated $CD4^+$ T cells. Indeed, as seen in Fig. 2*B*, pretreatment of these activated cells with FK506 and CsA both reduced the amount of ICOS mRNA up-regulation compared with untreated cells, indicating that this signaling pathway probably acts at the level of ICOS transcription.

In addition, we show that PP2 but not piceatannol also attenuated TCR/CD28-induced ICOS induction, hence implicating the Src rather than Syk family of protein-tyrosine kinases in regulating ICOS expression (Fig. 2*A*). Again, the regulation of ICOS by the Src family kinases appeared to be at the transcriptional level, since PP2-treated TCR/CD28-activated $CD4^+$ T cells had reduced levels of ICOS mRNA compared with control cells (Fig. 2*B*). To ascertain which of the Src kinases were involved (Fyn and Lck being the most highly expressed in T cells), we treated cells with damnacanthal, a highly potent and selective inhibitor of Lck activity (32). ICOS induction at both the cell surface protein and mRNA expression levels were unaltered by damnacanthal treatment, thus implicating Fyn but not Lck as the primary tyrosine kinase involved (Fig. 2, *A* and *B*). Although we could not rule out a possible role for Src kinase, our analysis of Fyn-deficient $CD4^+$ T cells indicate that Fyn probably plays a major role in inducing ICOS expression, since these cells expressed reduced levels of cell surface ICOS protein or ICOS mRNA compared with Fyn-sufficient cells upon TCR/CD28 stimulation (Fig. 2, *C* and *D*, respectively).

TCR/CD28 engagement is also known to activate the various mitogen-activated protein kinases (33). We found that ERK, but not JNK or p38 mitogen-activated protein kinase, played a critical role in ICOS induction. ICOS induction was virtually abrogated when TCR/CD28-activated $CD4^+$ T cells were pretreated with the ERK inhibitor, U0126, but not with the JNK inhibitor (L form) or p38 inhibitor, SB203580 (Fig. 2*A*, *middle*). This inhibition appeared to act also at the transcriptional level, similar to that mediated by CsA and PP2 (Fig. 2*B*).

Despite a number of studies emphasizing the importance of phosphatidylinositol-3-kinase in CD28 signaling leading to cell activation, proliferation, and survival (34–36), ICOS induction did not seem to be dependent on phosphatidylinositol 3-kinase or mTOR pathways, because treatment of cells with wortmannin or rapamycin, respectively, did not affect TCR/CD28-mediated ICOS up-regulation (Fig. 2*A*, *right*). We also did not observe any effect of SN-50 inhibitor peptide on ICOS induction, thus indicating a negligible or redundant role for NF-κB in TCR/CD28-mediated ICOS induction.

As a control to ensure that the dampening of ICOS induction by some of the chemical inhibitors examined above was not due to their effect on the surface expression of CD3 and/or CD28 molecules leading to diminution of ICOS induction, we treated $CD4^+$ T cells with these inhibitors for 16 h and found that the cell surface expression of CD3 and that of CD28 were unaffected by these inhibitors (data not shown).

Finally, we also addressed the feasibility of using the mouse EL4 T cell line as a model for subsequent study of ICOS regulation. Although there was already a high level of basal ICOS transcript in EL4 cells, the level of ICOS mRNA in these cells could be further elevated upon stimulation with TCR/CD28 or PMA and ionomycin (henceforth designated as P/I) (Fig. 2*E*) (data not shown). Importantly, as in primary $CD4^+$ T cells,

[4] The underlined sequences denote the mutant binding site for ERK-sensitive TF(s).

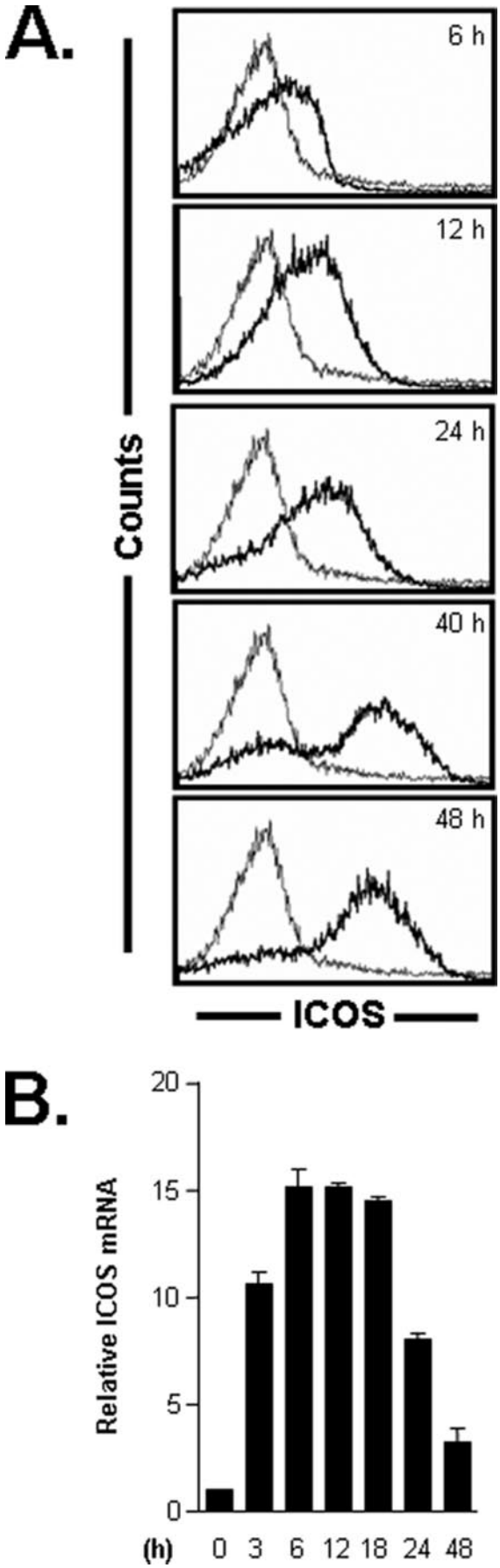

TCR/CD28-induced ICOS mRNA induction in EL4 cells could also be blocked by PP2, U0126, and CsA. Thus, taken together, our results using both murine primary $CD4^+$ T cells and EL4 T cells indicate that Fyn, calcineurin, and ERK are the primary signaling molecules involved in the induction of ICOS transcription upon TCR/CD28 stimulation.

Fyn Induces ICOS Transcription in Part through NFATc2 Independently of ERK—Since the above study with U0126 implicated ERK in TCR/CD28-mediated ICOS induction, we expressed a constitutively active form of MEK2 (caMEK2), which is the upstream kinase of ERK, in EL4 cells to determine if hyperactivation of ERK would result in enhanced ICOS induction. As shown in Fig. 3*A*, the expression of increasing amounts of caMEK2 resulted in a dosage-dependent induction of ICOS mRNA levels. This result, together with our previous data using U0126, unambiguously established a role for ERK in ICOS induction.

Since we demonstrated earlier that the signaling pathways leading to TCR/CD28-mediated ICOS induction were sensitive to CsA and FK506 (Fig. 2), we hypothesized that NFAT proteins could be involved in TCR/CD28-mediated ICOS induction. Three NFAT family members are expressed in T cells, namely NFATc1, NFATc2, and NFATc3 (37). As shown in Fig. 3*A*, overexpression of NFATc2 in P/I-treated EL4 cells led to a dramatic increase in ICOS mRNA levels, whereas the level of ICOS mRNA induction was modest or negligible in P/I-treated EL4 cells overexpressing NFATc1 or NFATc3, respectively. Thus, NFATc2 is involved in TCR/CD28-induced ICOS mRNA up-regulation.

The studies so far had indicated that Fyn, ERK, calcineurin, and NFATc2 were involved in TCR/CD28-mediated ICOS induction. However, within the TCR/CD28 signal transduction hierarchy, the participation of Fyn and ERK is proximal with respect to the downstream TF NFATc2. To determine if Fyn- or ERK-mediated ICOS induction occurs in part via NFATc2, we examined the effect of NFATc2 overexpression in TCR/CD28-stimulated EL4 cells pretreated with PP2 or U0126 (Fig. 3*C*). As expected, PP2 or U0126 treatment inhibited ICOS induction in TCR/CD28-stimulated EL4 cells. Interestingly, NFATc2 overexpression could overcome the dampening of ICOS induction in PP2-treated but not U0126-treated TCR/CD28-activated EL4 cells in a dose-dependent manner, suggesting that NFATc2 is probably downstream of Fyn but not ERK in inducing ICOS transcription.

NFATc2 resides in the cytoplasm and translocates to the nucleus upon activation (38). Consistent with the above finding that NFATc2 is downstream of Fyn but not ERK signaling, we also found that PP2 but not U0126 pretreatment of TCR/CD28-stimulated EL4 cells resulted in a reduction of NFATc2 trans-

FIGURE 1. **ICOS expression is induced at the transcriptional level upon T cell activation.** *A*, purified murine primary $CD4^+$ T cells were stimulated with plate-bound anti-CD3 (1 μg/ml) and soluble anti-CD28 (4 μg/ml) antibodies for various times as indicated and analyzed for cell surface expression of ICOS by flow cytometry. ICOS expression on stimulated cells (*thick line*) is compared with that of unstimulated cells at 0 h (*thin line*). Data shown are representative of two independent experiments. *B*, ICOS mRNA levels in T cells activated for various times were analyzed by quantitative real time RT-PCR. Data shown had been normalized to those from unstimulated cells at 0 h and were expressed as mean values ± S.E. of at least two independent experiments.

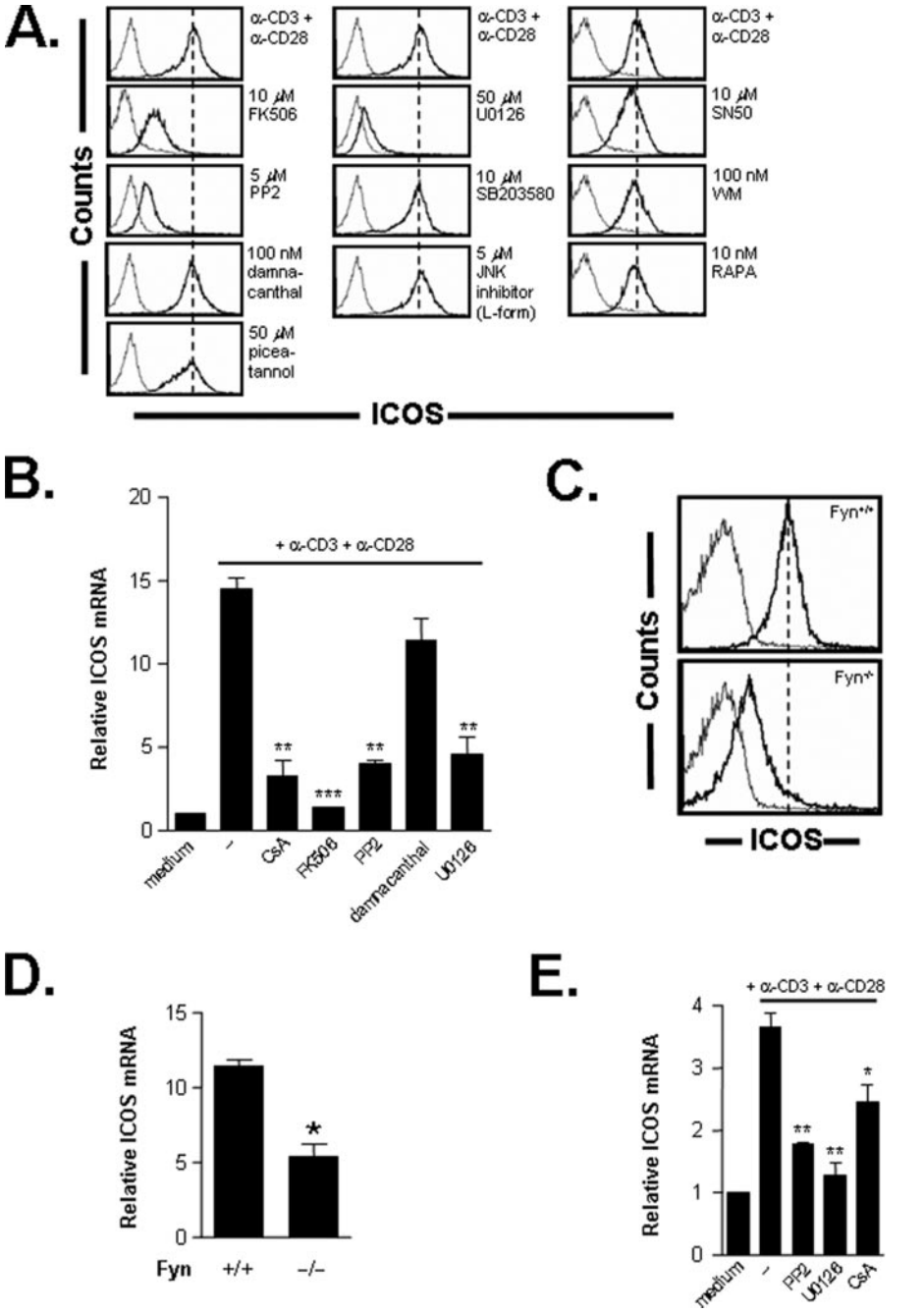

FIGURE 2. **ICOS induction by TCR and CD28 engagement is regulated by distinct downstream signaling pathways.** *A*, ICOS induction on activated $CD4^+$ T cells pretreated with various chemical inhibitors. Purified $CD4^+$ T cells were pretreated with various inhibitors for 1 h and stimulated as in Fig. 1 for 40–48 h prior to examination of surface ICOS expression via flow cytometry (*thick* and *thin lines* are as depicted in Fig. 1). Data shown are representative of two independent experiments. *B*, measurement of ICOS mRNA level in activated $CD4^+$ T cells pretreated with inhibitors. Cells were stimulated as above and harvested 6 h later to assess ICOS mRNA level by real time RT-PCR. Data were normalized to those from unstimulated cells and shown as mean ± S.E. of at least two independent experiments. *C* and *D*, purified $CD4^+$ T cells from $Fyn^{+/+}$ and $Fyn^{-/-}$ mice were stimulated and harvested as in Fig. 1. Cell surface ICOS expression and ICOS mRNA level were assessed by flow cytometry and real time RT-PCR, respectively. Data shown are mean values ± S.E. of two independent experiments. *E*, murine EL4 thymoma cells were treated as in *A* and harvested after 14–16 h, and ICOS mRNA levels were quantified by real time RT-PCR. *, $p < 0.05$; **, $p < 0.01$; ***, $p < 0.001$. *RAPA*, rapamycin; *WM*, wortmannin.

location into the nucleus compared with untreated or U0126-treated cells that were subjected to the same stimulus (Fig. 4*A*).

Although most studies of TCR signaling have positioned ERK downstream of Fyn in the TCR signalosome, our data seem to indicate that ERK acts in a signaling axis distinct from Fyn in regulating ICOS upon TCR/CD28 stimulation. To further clarify this, we examined ERK activation in the absence of Fyn signaling in EL4 cells. As shown in Fig. 4*B*, ERK activation in TCR/CD28-stimulated EL4 cells, with or without PP2 pretreatment, was comparable (Fig. 4*B*). This is consistent with previous work showing the same between $Fyn^{+/+}$ and $Fyn^{-/-}$ $CD4^+$ T cells (39). It is therefore apparent that Fyn does not act through ERK to initiate ICOS transcription and that ERK acts in an independent signaling pathway to regulate ICOS. Collectively, our data demonstrate that Fyn-calcineurin-NFATc2 and MEK2-ERK1/2 pathways signal independently to activate ICOS transcription.

A 288-bp Core Promoter Region of icos Confers PMA and Ionomycin-induced Expression of a Reporter in Vitro—To further elucidate the molecular mechanisms leading to *icos* promoter activation, we first tested a 1.48-kb KpnI-HindIII fragment 5′ of the TSS of the mouse *icos* gene for possession of promoter activity. This fragment was linked in the sense orientation to the promoterless luciferase (Luc) reporter vector pGL3B to create mICOSp(−1478)-Luc, which was transiently cotransfected with a normalization vector, pRL-*Renilla*, into EL4 cells. Subsequently, cells were left in medium alone or stimulated with P/I and, after a further 14–16 h of incubation, harvested and evaluated for Luc activity. P/I were used instead of anti-CD3 and anti-CD28 antibodies for stimulating cells, since the former treatment gave a larger -fold increase in luciferase activity compared with the latter (data not shown).

As seen in Fig. 5*A*, the *icos* 5′ 1.48-kb DNA fragment conferred significant Luc activity in stimulated EL4 cells. There was an ~61-fold induction in Luc activity in cells stimulated with P/I compared with cells in medium only. As a control, insertion of the same promoter fragment in the antisense orientation resulted in a complete loss of its ability to activate the reporter construct (data not shown). Thus, the data indicate that the 1.48-kb region upstream of *icos* TSS contains significant promoter activity.

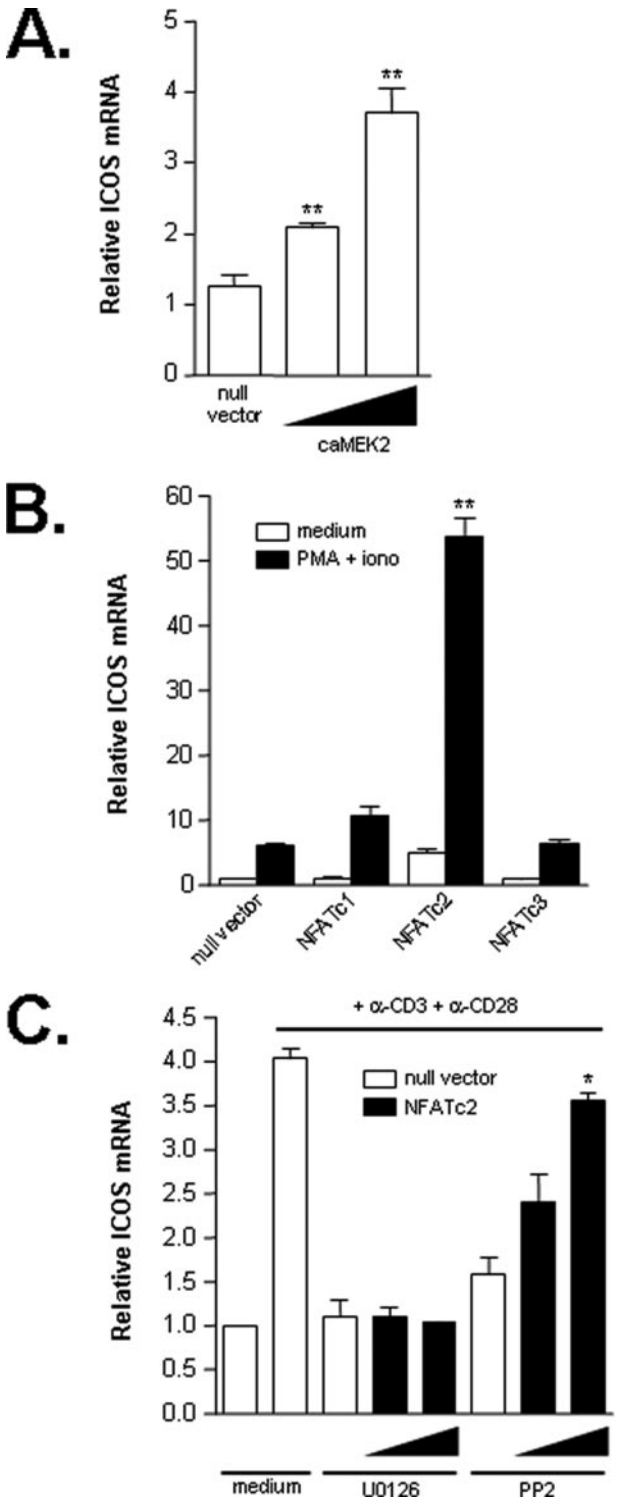

FIGURE 3. **Induction of ICOS transcription by ectopic expression of MEK2 and NFATc2.** *A*, EL4 cells were transfected with a null vector or increasing amounts of constitutively active MEK2 (caMEK2), and the amount of ICOS mRNA was quantified by real time RT-PCR. **, $p < 0.001$. *B*, EL4 cells were transfected with vectors expressing NFATc1, NFATc2, or NFATc3 and were either left unstimulated (*white bars*) or stimulated with PMA and ionomycin (*black bars*) and examined for ICOS mRNA levels via RT-PCR. **, $p < 0.001$. *C*, EL4 cells transfected with null vector (*white bars*) or NFATc2 vector (*black bars*) were pretreated with U0126 or PP2 and stimulated with anti-CD3 and anti-CD28 antibodies, and their ICOS mRNA levels were assessed by real time RT-PCR. Data were normalized to cells transfected with null vector and shown as mean ± S.E. of two independent experiments. *, $p < 0.05$.

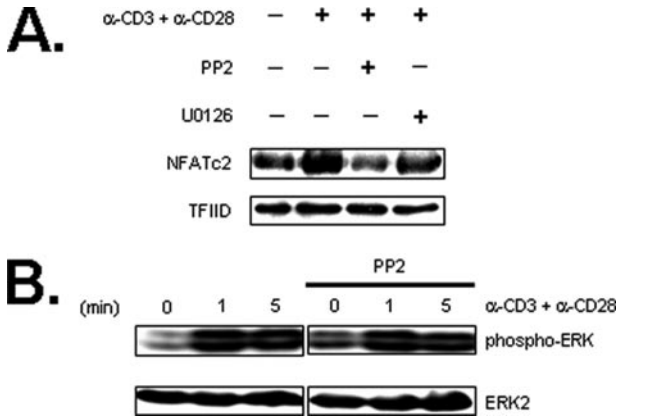

FIGURE 4. **PP2 treatment affects NFATc2 nuclear translocation but not ERK activation.** *A*, EL4 cells were untreated or pretreated with PP2 or U0126 and subsequently stimulated with anti-CD3 and anti-CD28 antibodies for 16 h. Nuclear extracts (10 μg) were subjected to immunoblotting with anti-NFATc2 monoclonal antibody. The anti-TFIID blot serves as control for equal loading of extracts. *B*, EL4 cells were either untreated or pretreated with PP2 and then stimulated for the times indicated. ERK activation was assessed by Western blotting using anti-phospho-ERK antibody and the anti-ERK2 blot serves as a loading control.

To define more specifically the elements contributing to *icos* promoter activity, we generated a series of promoter mutants by truncating the 1.48-kb DNA fragment from the 5′ end. Whereas the 900-bp BglII-HindIII (−900 to −1) and the 599-bp XhoI-HindIII (−599 to −1) fragments retained promoter activity, additional deletion of the *icos* promoter revealed that a 288-bp fragment was the minimum region responsible for substantial transcriptional activating capability associated with the 1.48-kb parental fragment. A further 5′ truncation yielding a 147-bp fragment resulted in dramatic reduction of promoter activity (~10-fold loss in Luc activity), and subsequent deletions leading to 109- and 52-bp fragments led to an almost complete loss of promoter activity (Fig. 5*A*). Hence, based on these *in vitro* luciferase reporter assays, we concluded that the 288-bp region upstream of the *icos* TSS was the minimum DNA region that retained significant promoter activity capable of conferring a high level of ICOS transcription.

Requirement of NFATc2 and ERK-dependent Transcription Factor(s) for icos Core Promoter Activity—We next asked if Fyn-NFATc2 and ERK signaling cascades could influence the core promoter activity of *icos*. To this end, we assessed the effects of CsA and U0126 treatment on the promoter activity of the 288-, 147-, and 109-bp DNA fragments of *icos*. We observed that CsA treatment reduced markedly the reporter activity of the 288-bp but not the 147-bp fragment following transient cotransfection of mICOSp(−288)-Luc, mICOSp(−147)-Luc, or mICOSp(−109)-Luc and pRL-*Renilla* in EL4 cells (Fig. 5*B*, *left*). In contrast, U0126 treatment virtually obliterated the promoter activities of both the 288- and 147-bp fragments, suggesting that ERK signaling has a very profound effect on the activation status and/or DNA binding activity of potential TFs that recognize the *cis*-regulatory elements within the 147-bp region (Fig. 5*B*, *right*). In addition, our data suggest that CsA-sensitive TFs, such as NFAT, probably act within the region between 288 and 147 bp upstream of *icos* TSS.

To further support the findings that ERK and NFAT signaling are involved in the induction of ICOS transcription through spe-

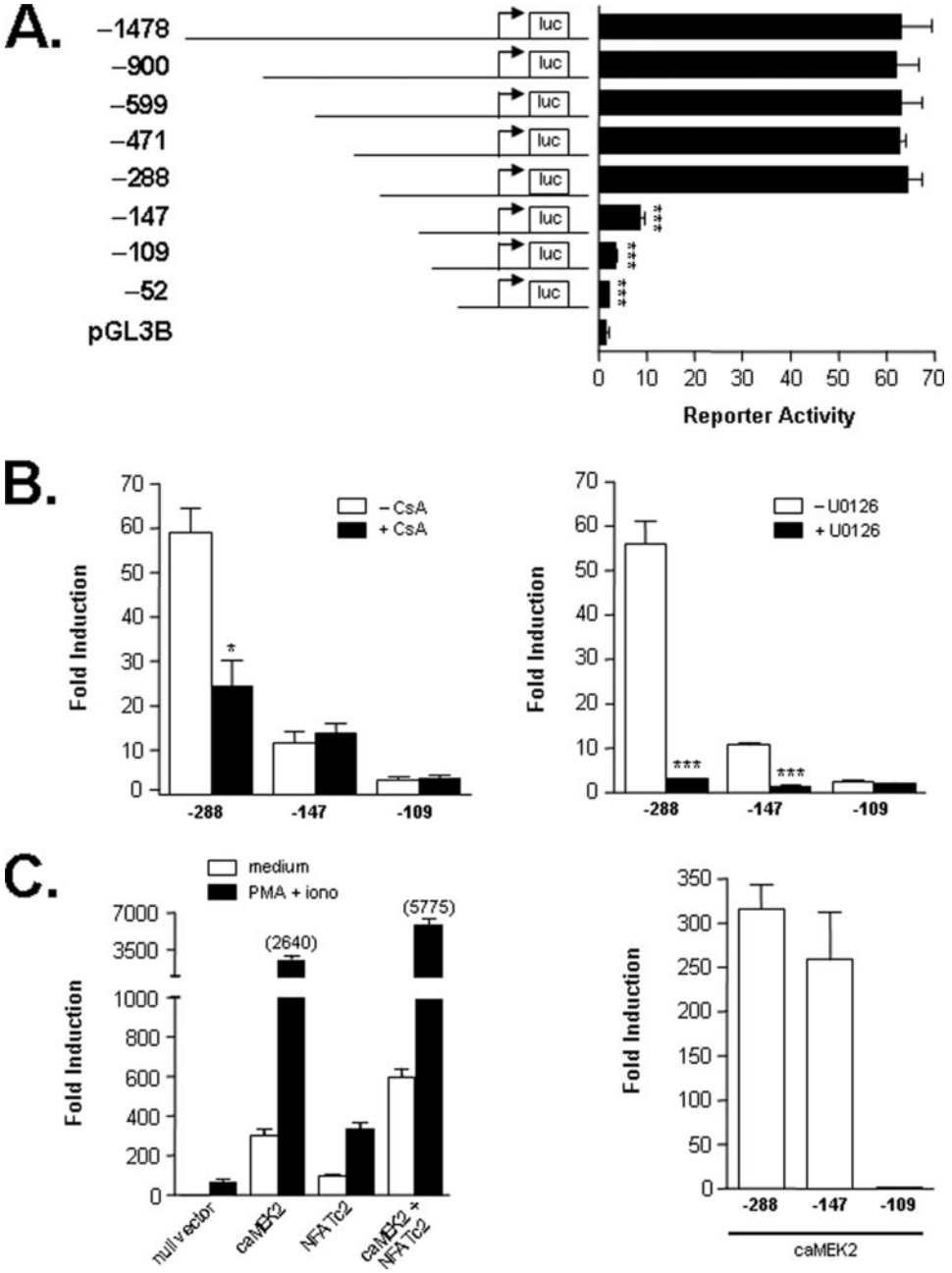

FIGURE 5. **Transactivation of the putative *icos* promoter by NFATc2 and ERK signaling.** *A*, delineation of the minimal *icos* promoter. A series of 5′ truncations of the *icos* promoter was created as shown and linked to a luciferase reporter gene and transfected into EL4 cells, which were subsequently stimulated with PMA + ionomycin. -Fold induction of luciferase activity was calculated as the ratio of the normalized luciferase activity of stimulated cells to unstimulated cells. *B*, the activity of the putative *icos* promoter is affected by CsA and U0126 treatment. EL4 cells were transfected in triplicate with mICOSp(−288)-Luc, mICOSp(−147)-Luc, or mICOSp(−109)-Luc constructs and stimulated with PMA and ionomycin in the absence (*white bars*) or presence (*black bars*) of 50 ng/ml CsA (*left*) or 50 μM U0126 (*right*). *C*, ectopic expression of a constitutively active MEK2 or NFATc2 transactivates the minimal *icos* promoter. EL4 cells were transfected in triplicate with mICOSp(−288)-Luc (*left and right*), mICOSp(−147)-Luc, or mICOSp(−109)-Luc (*right*) together with the indicated expression vectors. Cells were either unstimulated (*white bars*) or stimulated with PMA + ionomycin (*black bars*) for 16 h. -Fold induction was calculated as the ratio of normalized luciferase activity of cells overexpressing the stated protein(s) to cells transfected with null vector. Data shown are mean ± S.E. of triplicate samples and representative of two independent experiments. *, $p < 0.05$; ***, $p < 0.001$. *iono*, ionomycin.

cific action within the 288-bp promoter region, we overexpressed individually caMEK2 and NFATc2 in cells harboring mICOSp(−288)-Luc. Both caMEK2 and NFATc2 could enhance the promoter activity of mICOSp(−288)-Luc (Fig. 5*C*, *left*). Strikingly, cotransfection of both led to a synergistic amplification of promoter activity, suggesting the possibility of cooperation between the ERK-responsive TFs and NFATc2 in accentuating *icos* promoter activity. Thus, ERK and NFATc2 could cooperatively activate the *icos* promoter. Furthermore, consistent with the data shown in Fig. 5*B*, overexpression of caMEK2 could also enhance the promoter activity of mICOSp(−147)-Luc (but not mICOSp(−109)-Luc) comparable with that of mICOSp (−288)-Luc, indicating that the ERK-responsive TFs act in this region of the promoter (Fig. 5*C*, *right*).

NFATc2 Binds icos 288-bp Core Promoter in Vivo and Is Affected by Fyn Signaling—In order to delineate the *cis*-regulatory elements contributing to *icos* core promoter activity, we proceeded to search for putative TF-binding sites within the 288-bp region by employing the World Wide Web-based software, MATINSPECTOR (available on the World Wide Web at www.genomatix.de) and RVISTA 2.0 (available on the World Wide Web at rvista.dcode.org) (40, 41), which are closely interconnected with the TRANSFAC data base. These programs predicted the presence of potential AP1, CCAAT/enhancer-binding protein β and Ikaros but, surprisingly, not NFATc binding sites, although we showed an important role for NFATc2 in activating the *icos* promoter. From the algorithmic predictions, we postulated that AP1 could be another TF candidate that regulates ICOS expression, since c-*fos* was directly downstream of ERK in many signaling pathways. However, preliminary experiments exploring site-directed mutagenesis of the putative AP1 site (and other sites) within mICOSp(−288)-Luc did not lead to reproducible reduction in Luc reporter activity. Conversely, overexpression of c-*fos* did not further enhance Luc activity in EL4 cells cotransfected with mICOSp(−288)-Luc (data not shown).

Since NFATc2 overexpression resulted in increased mICOSp(−288)-Luc activity (Fig. 5*C*, *left*), we asked if NFATc2 could bind the 288-bp fragment *in vivo*. Using ChIP assays, we detected a basal level of constitutive binding of NFATc2 to the *icos* promoter in resting EL4 cells (Fig. 6*A*, *top*, *lane 5*), possibly

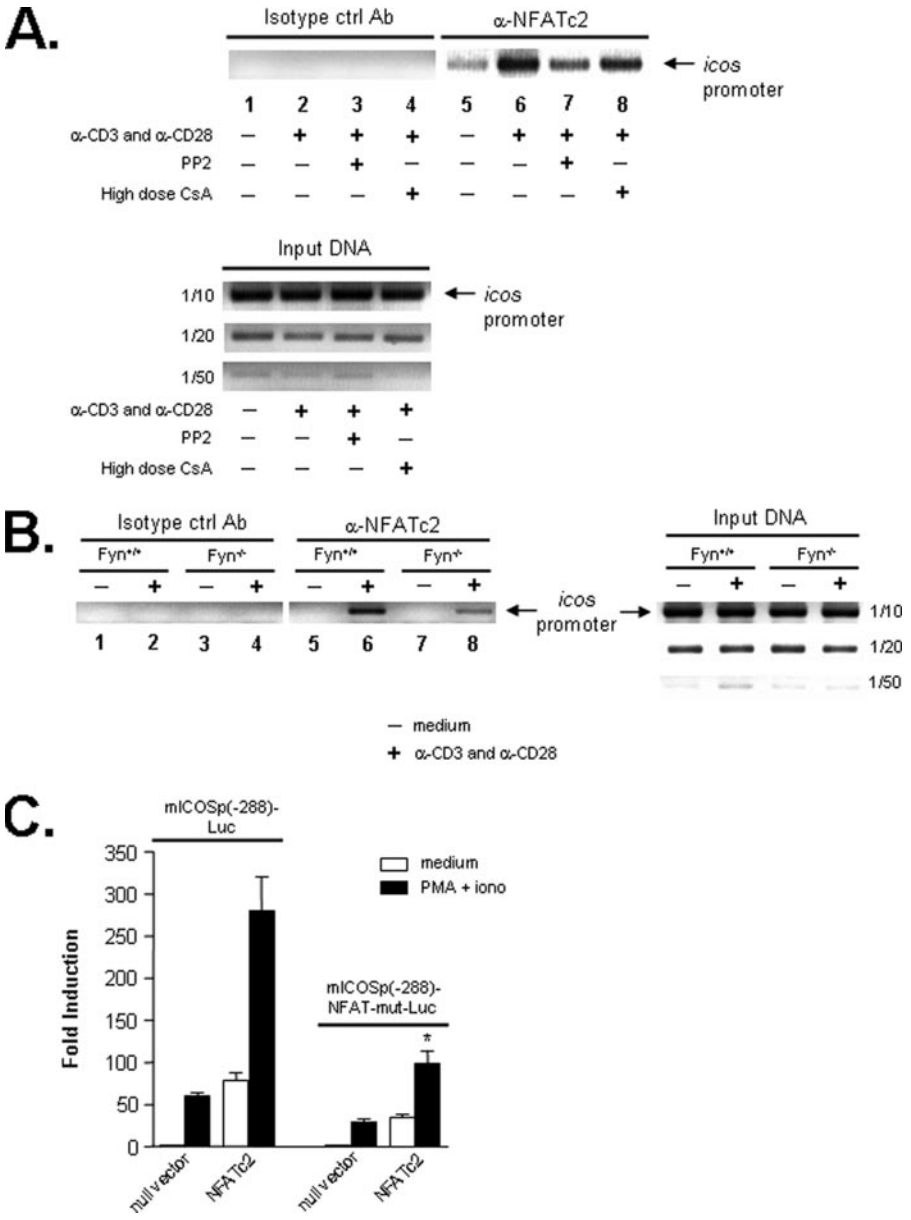

FIGURE 6. **CHIP analyses of NFATc2 binding to the *icos* minimal promoter.** *A*, EL4 cells, either untreated or pretreated with the indicated inhibitors for 1 h, were transfected with NFATc2 vector before stimulation with anti-CD3 and anti-CD28 antibodies for 16 h. Chromatin complexes were immunoprecipitated with either isotype control (*top*, *lanes 1–4*) or anti-NFATc2 antibody (*top*, *lanes 5–8*), and PCR analyses of the region between −288 and −1 of the *icos* promoter were done on the precipitated DNA. To assess for equivalent loading of substrates, the same PCR was performed on serially diluted DNA before immunoprecipitation (*bottom*). -Fold dilutions of templates are indicated on the *left*. *B*, lack of Fyn signaling affects NFATc2 binding to the minimal *icos* promoter. Purified $CD4^+$ T cells from $Fyn^{+/+}$ and $Fyn^{-/-}$ mice were either unstimulated or stimulated with anti-CD3 and anti-CD28 antibodies for 16 h, and ChIP was performed as in *A*. Results are representative of at least two independent experiments. *C*, EL4 cells co-transfected in triplicate with mICOSp(−288)-Luc or mICOSp(−288)-NFAT-mut-Luc and NFATc2 were either unstimulated (*white bars*) or stimulated with PMA and ionomycin (*black bars*). -Fold induction was quantitated as in Fig. 5*C*. Data shown are mean ± S.E. of triplicate samples and representative of two independent experiments.

as a result of deregulated Ca^{2+} signaling in these cells (42). Importantly, this level of binding was substantially increased when EL4 cells were stimulated with anti-CD3 and anti-CD28 antibodies (*lane 6*). PP2 treatment on similarly stimulated cells resulted in a reduction in NFATc2 binding (*lane 7*), suggesting that the positive impact of Fyn signaling on ICOS transcription observed earlier is via enhancing NFATc2 binding of the *icos* 288-bp promoter. As a positive control, CsA treatment was also observed to diminish, although not to the same extent, NFATc2 binding (*lane 8*). Binding of NFATc2 to the *icos* promoter was specific, since ChIP performed using an isotype-matched antibody did not produce visible PCR products (*lanes 1–4*). We also examined the binding of NFATc2 to the *icos* promoter in primary $CD4^+$ T cells lacking Fyn (Fig. 6*B*). Consistent with the finding that Fyn and NFATc2 act in the same signaling axis to activate ICOS transcription, we show that there was reduced binding of NFATc2 to the *icos* promoter in Fyn-deficient $CD4^+$ T cells activated by anti-CD3 antibodies and anti-CD28 antibodies (*lane 8 versus lane 6*). NFATc2 appeared to occupy a region encompassing bp 230–234 of the *icos* promoter, because mutation of the bases between bp 232 and 231 led to a potent reduction in promoter activity when NFATc2 was overexpressed (compare Luc activity due to mICOSp(−288)-Luc with that due to mICOSp(−288)-NFAT-mut-Luc in Fig. 6*C*).

Identification of an ERK-responsive Site in the icos Promoter—Since treatment with U0126 affected ICOS induction in TCR/CD28-stimulated T cells, and this effect appeared to be at the promoter level, we sought to identify potential ERK-responsive site(s) within the *icos* core promoter region. To this end, we designed a set of double-stranded oligonucleotides that overlapped each other and spanned the region from bp 154 to 105 upstream of the *icos* TSS and used them to compete against nuclear extract binding by this region. As shown in Fig. 7*A*, *left*, EMSA performed with nuclear extracts obtained from P/I-stimulated EL4 cells demonstrated significant nuclear complex binding of the *icos* promoter region spanning bp 154 to 105 (*lane 2*). Although molar excess of the unlabeled oligonucleotide spanning bp 129 to 105 (p129_105) failed to compete with the radiolabeled p154_105 (*lane 5*), the unlabeled p154_130 did (*lane 4*), suggesting that the region between 154 and 130 bp upstream of *icos* TSS very likely bound nuclear protein. Using a series of 3-bp scrambled mutations along the length of bp 154 to 130, we refined the position of the binding site to between bp 148 and 136 (data not shown). Moreover, the

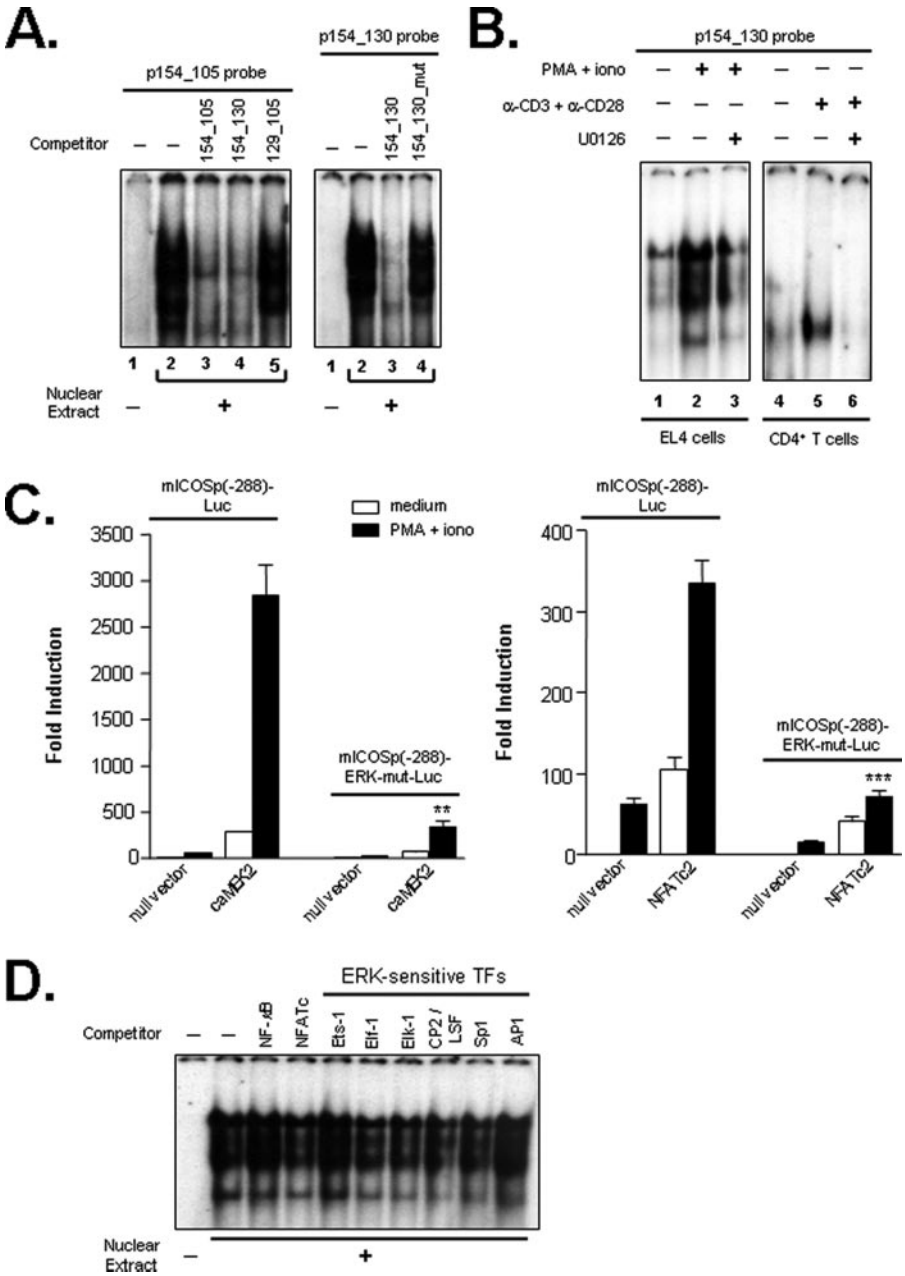

FIGURE 7. **Identification of an ERK-sensitive site on the *icos* promoter.** *A*, demonstration of specific transcriptional complex binding to DNA region −154 to −130 of *icos* promoter. Radiolabeled double-stranded oligonucleotides, p154_105 and p154_130, were incubated with nuclear extracts from P/I-stimulated EL4 cells either in the presence or absence of excess unlabeled competitors (*left* and *right panels*) and analyzed via EMSA. *B*, demonstration that the transcriptional complex binding the p154_130 probe is sensitive to ERK inhibitor. The p154_130 probe was incubated with nuclear extracts from EL4 cells (*lanes 1–3*) or CD4$^+$ T cells (*lanes 4–6*) that were untreated or treated as stated in the figure and subjected to EMSA. *C*, EL4 cells were co-transfected in triplicate as in Fig. 6*C* but with mICOSp(−288)-ERK-mut-Luc and caMEK2 (*left*) or NFATc2 (*right*). *D*, the p154_130 probe was incubated with nuclear extracts from PMA and ionomycin-stimulated EL4 cells in the presence or absence of excess unlabeled competitors bearing the consensus binding sites of members of various transcription factor families; in particular, those that are known to act downstream of ERK. **, $p < 0.01$; ***, $p < 0.001$. *iono*, ionomycin.

introduction of a 3-bp mutation corresponding to bp 144 to 142 of p154_130 (p154_p130_mut) interfered largely with the ability of unlabeled p154_130_mut to compete with the radiolabeled p154_130 (Fig. 7*A*, *right*, *lane 4*), suggesting that the integrity of this site is important to facilitate optimal binding of as yet undetermined nuclear factors. EMSAs revealed that there was considerable induction of complex binding of the stated region to nuclear extracts obtained from either P/I-stimulated EL4 cells or TCR/CD28-activated murine primary CD4$^+$ T cells compared with those of resting cells (Fig. 7*B*, *lanes 2* and *5*, respectively). This binding was reduced dramatically or abrogated in activated EL4 and CD4$^+$ T cells pretreated with U0126 (*lanes 3* and *6*, respectively).

To definitively confirm the functional relevance of the region spanning bp 154 to 130 upstream of the *icos* TSS in responding to ERK signaling, we replicated the above described mutation spanning bp 144 to 142 in the mICOSp(−288)-Luc construct to yield mICOSp(−288)-ERK-mut-Luc and assessed the latter's reporter activity in EL4 cells ectopically expressing constitutively active MEK2. Consistent with our previous result demonstrating compromised nuclear complex binding, the introduced mutation in mICOSp(−288)-Luc led accordingly to a drastic reduction in Luc activity (Fig. 7*C*, *left*). Interestingly, a drastic attenuation in Luc activity was also observed in EL4 cells overexpressing NFATc2 (Fig. 7*C*, *right*), alluding to a possible functional hierarchy involving ERK-sensitive TFs and NFATc2, whereby the latter critically requires the former to operate, otherwise its own function is crippled. In other words, ERK signaling appeared to be extremely important in initiating or sustaining basal ICOS transcription, whereas NFATc2 as well as other possible TFs played a more ancillary role in amplifying transcription. This finding is consistent with the failure of exogenous NFATc2 to rescue ICOS transcription in U0126-treated EL4 cells (Fig. 3*C*) and the earlier purported cooperativity of ERK and NFATc2 signaling in driving ICOS induction (Fig. 5*C*, *left*).

Since the region spanning bp 154 to 130 was responsive to ERK signaling, we attempted to identify the TF(s) that binds this region. For this purpose, we designed a series of unlabeled oligonucleotides bearing consensus DNA sequences that were known and had been shown to bind various ERK-sensitive TFs, such as Ets-1, Elf-1, Elk-1, CP2 or LSF, Sp1, and AP1 as well as those recognizing NFATc and NF-κB and used these to compete with the binding of nuclear extracts from activated EL4 or CD4$^+$ T

cells to the *icos* promoter. None of these unlabeled oligonucleotides convincingly competed with the radiolabeled p154_130 in binding the protein complex from activated EL4 or $CD4^+$ T cells (Fig. 7*D*). Furthermore, the DNA-protein complex did not supershift with either anti-c-*fos* or anti-c-*jun* Abs (data not shown). Thus, at this juncture, we are unable to ascertain the identity of the TF(s), except to report that it was responsive to ERK.

DISCUSSION

ICOS is a member of the CD28 superfamily of costimulatory receptors that is expressed at low levels on naive T cells but rapidly up-regulated on activated T cells. Although the *in vivo* functions of ICOS in health and disease are quite well understood, very little is known about the molecular mechanisms that regulate ICOS expression. In this study, we present evidence that the Fyn-calcineurin-NFATc2 and MEK2-ERK1/2 signaling pathways directly induce ICOS expression upon TCR and CD28 co-stimulation of T cells.

We first demonstrated that there was a direct correlation between the up-regulation of ICOS cell surface expression and the induction of its mRNA, suggesting that TCR/CD28 signaling directly regulates ICOS expression at the transcriptional level. Both TCR and CD28 stimulation are known to activate a number of downstream signaling molecules, and it is expected that not all of them are involved in regulating ICOS. T cells possess both the Syk and Src family of tyrosine kinases, which are important in proximal TCR signaling. Our data indicate that Src family tyrosine kinases play a major role in TCR-mediated ICOS induction. Of the two major Src kinases present in T cells, namely Lck and Fyn, the latter seems to be critical for inducing ICOS. This demonstrates a nonredundancy of the two kinases in an important aspect of T cell physiology.

Consistent with the fact that CD28 co-stimulation is known to activate the NFAT family of transcription factors, our results clearly demonstrate an important role for NFATc2 in activating ICOS transcription (Figs. 3, 5, and 6). TCR engagement is known to activate the Ca^{2+}/calmodulin-dependent serine phosphatase, calcineurin, which dephosphorylates NFAT proteins and leads to their translocation into the nucleus. Nuclear NFAT has been shown to activate cytokine gene (*e.g.* IL-2) promoters and enhancers, resulting in positive T cell responses (reviewed in Refs. 43 and 44). Our studies expand these previous findings and implicate an additional nontrivial role for the calcineurin-NFATc2 pathway in up-regulating ICOS transcription. This was supported by our data showing the ability of the immunosuppressive drug CsA in blocking ICOS induction at both the cell surface receptor and mRNA levels (Fig. 2, *A*, *B*, and *E*) and affecting *icos* promoter activity (Fig. 5*B*, *left*). Moreover, exogenously expressed NFATc2 could enhance ICOS mRNA levels (Fig. 3*B*) and promoter activity (Fig. 5*C*, *left*). Thus, NFATc2 is involved in the regulating ICOS expression.

The attenuation of NFATc2 nuclear translocation and *in vivo* occupation of the *icos* promoter region following PP2 treatment of activated T cells and the ability of NFATc2 overexpression to overcome PP2 inhibition of ICOS induction in activated EL4 cells places NFATc2 downstream of Fyn in the signaling axis that induces ICOS expression. Indeed, evidence that the binding of the *icos* promoter by NFATc2 is compromised in $Fyn^{-/-}$ $CD4^+$ T cells provided further support for this notion of a Fyn-calcineurin-NFATc2 signaling axis that regulates ICOS transcription.

Other major pathways activated by TCR and CD28 signaling include those involving mitogen-activated protein kinases, of which ERK appeared to play a major role in ICOS induction. This is inferred from the efficiency of the pharmacological inhibitor U0126 (but not p38 inhibitor SB203580 or JNK inhibitor I) in blocking ICOS receptor (Fig. 2*A*) and mRNA (Fig. 2, *B* and *E*) up-regulation, as well as almost ablating *icos* promoter activity (Fig. 5*B*, *right*). Cotransfection assays with a constitutively active form of MEK2 (caMEK2) demonstrated that overexpressed caMEK2 enhanced ICOS transcription (Fig. 3*A*) and promoter activity (Fig. 5*C*). Although we eventually identified a functional target site residing within bp 148 to 136 of the *icos* promoter region responsive to ERK signaling (because mutation of this site severely dampened reporter activity in caMEK2-overexpressed EL4 cells (Fig. 7*D*)), the identity of the TF(s) that binds this region is far from clear. Further investigation has to be carried out to determine the identity of this TF(s).

Our current findings also seem to suggest that ERK signaling independently and critically regulates ICOS expression, since the overexpression of NFATc2 could not rescue the U0126-mediated block in ICOS induction (Fig. 3*C*). Intriguingly, the ERK-responsive TF(s) appeared to occupy an *icos* promoter region that is different from that recognized by NFATc2. The overexpression of NFATc2 and caMEK2 synergistically induce ICOS expression at the mRNA level. Finally, mutation of the ERK-sensitive site within the *icos* promoter not only significantly impaired the ability of ERK but also NFATc2 in driving high levels of ICOS transcription. These data collectively support a model of two signaling pathways, namely Fyn-calcineurin-NFATc2 and MEK2-ERK1/2, that independently converge on the *icos* promoter to regulate transcription, with the added complexity that whereas ERK signaling is critical in initiating ICOS transcription, NFATc2 augments this ERK-mediated signal.

The study of the transcriptional regulation of ICOS is of immense importance, since the human chromosome region 2q33 that harbors the costimulatory cluster of CD28, ICOS, and CTLA-4 genes has been linked to a number of autoimmune diseases. Sequence alignment of regions flanking the first coding exon of the mouse and human *icos* genomic DNA revealed two zones of sequence homology separated by an ~250-bp mouse-specific repetitive DNA region (45). Interestingly, we found that the 288-bp region defined in this report to possess promoter activity is located within the mouse-specific repetitive region, implying possible differences in the regulation of mouse as compared with human ICOS transcription. Indeed, whereas ICOS plays an important role in the development of (and is preferentially expressed in) mouse Th2 cells (46, 47), its expression appears to be enhanced in human Th1 cells (48), although a recent study determined that polymorphisms in the human ICOS promoter are significantly associated with allergic sensitization and Th2 cytokine production (49). Thus, it is conceivable that differences in ICOS expression, brought about by differences in its transcriptional regulation, could

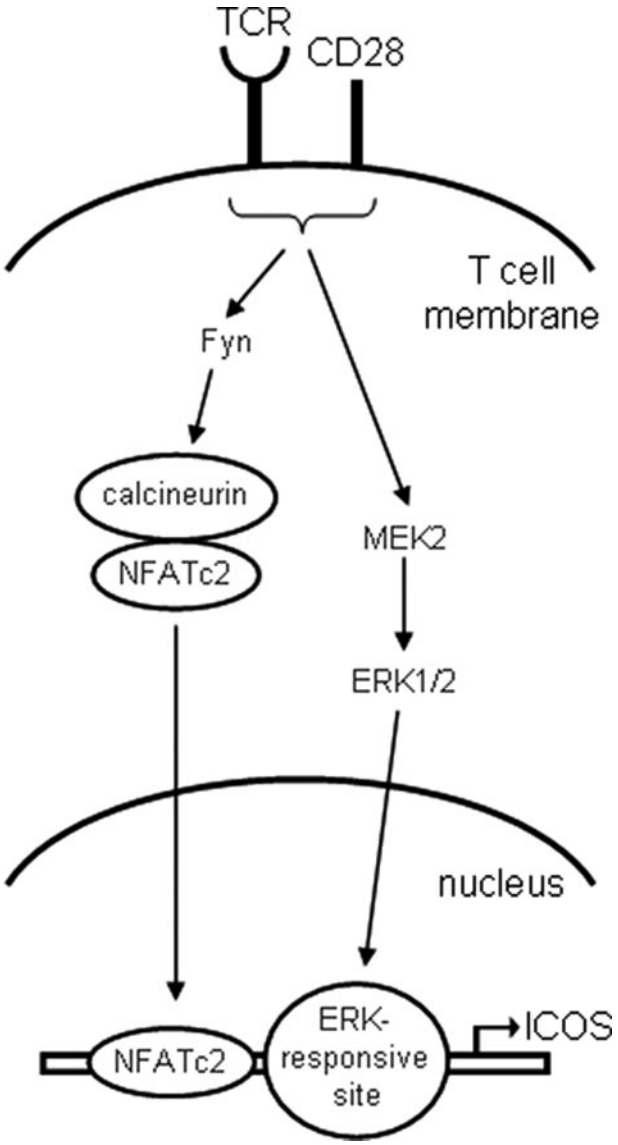

FIGURE 8. **Proposed model for transcriptional regulation of ICOS expression by Fyn-calcineurin-NFATc2 and MEK2-ERK1/2 signaling in T cells.**

influence immune responses in allergic, autoimmune, and disease conditions.

Because ICOS plays an important role in the pathogenesis of many diseases, understanding the molecular mechanisms by which ICOS is regulated may present new opportunities for therapeutic intervention of pathologies involving this costimulatory molecule. In this regard, our current studies could shed light on human studies investigating the association of autoimmune diseases, such as multiple sclerosis and type I diabetes with polymorphisms in the CD28/CTLA4/ICOS gene cluster.

In summary, this work has defined two molecular pathways downstream of TCR and CD28 signaling, namely Fyn-calcineurin-NFATc2 and MEK2-ERK1/2, in the regulation of mouse ICOS transcription (Fig. 8). Furthermore, we demonstrated the binding of ICOS promoter by NFATc2 and delineated an ERK-responsive site in the promoter, which probably binds yet to be identified TF(s). Future work will center on discovering other possible signaling pathways and TFs that regulate ICOS expression, especially those signaling pathways associated with the polarization of T cells into different T cell subsets.

Acknowledgments—We thank Weng-Keong Chew and You-Bin Lin for technical assistance and members of the LAM laboratory for critical comments regarding this project. We also thank the staff of the Singapore Biological Resource Centre for care and maintenance of mice.

REFERENCES

1. Chambers, C. A. (2001) *Trends Immunol.* **22,** 217–223
2. Frauwirth, K. A., and Thompson, C. B. (2002) *J. Clin. Invest.* **109,** 295–299
3. Civil, A., and Verweij, C. L. (1995) *Res. Immunol.* **146,** 158–164
4. Burr, J. S., Savage, N. D., Messah, G. E., Kimzey, S. L., Shaw, A. S., Arch, R. H., and Green, J. M. (2001) *J. Immunol.* **166,** 5331–5335
5. Whitmire, J. K., and Ahmed, R. (2000) *Curr. Opin. Immunol.* **12,** 448–455
6. Schweitzer, A. N., Borriello, F., Wong, R. C., Abbas, A. K., and Sharpe, A. H. (1997) *J. Immunol.* **158,** 2713–2722
7. London, C. A., Lodge, M. P., and Abbas, A. K. (2000) *J. Immunol.* **164,** 265–272
8. Lucas, P. J., Negishi, I., Nakayama, K., Fields, L. E., and Loh, D. Y. (1995) *J. Immunol.* **154,** 5757–5768
9. Beier, K. C., Hutloff, A., Dittrich, A. M., Heuck, C., Rauch, A., Buchner, K., Ludewig, B., Ochs, H. D., Mages, H. W., and Kroczek, R. A. (2000) *Eur. J. Immunol.* **30,** 3707–3717
10. Hutloff, A., Dittrich, A. M., Beier, K. C., Eljaschewitsch, B., Kraft, R., Anagnostopoulos, I., and Kroczek, R. A. (1999) *Nature* **397,** 263–266
11. Swallow, M. M., Wallin, J. J., and Sha, W. C. (1999) *Immunity* **11,** 423–432
12. Yoshinaga, S. K., Whoriskey, J. S., Khare, S. D., Sarmiento, U., Guo, J., Horan, T., Shih, G., Zhang, M., Coccia, M. A., Kohno, T., Tafuri-Bladt, A., Brankow, D., Campbell, P., Chang, D., Chiu, L., Dai, T., Duncan, G., Elliott, G. S., Hui, A., McCabe, S. M., Scully, S., Shahinian, A., Shaklee, C. L., Van, G., Mak, T. W., and Senaldi, G. (1999) *Nature* **402,** 827–832
13. Gonzalo, J. A., Tian, J., Delaney, T., Corcoran, J., Rottman, J. B., Lora, J., Al Garawi, A., Kroczek, R., Gutierrez-Ramos, J. C., and Coyle, A. J. (2001) *Nat. Immunol.* **2,** 597–604
14. Coyle, A. J., Lehar, S., Lloyd, C., Tian, J., Delaney, T., Manning, S., Nguyen, T., Burwell, T., Schneider, H., Gonzalo, J. A., Gosselin, M., Owen, L. R., Rudd, C. E., and Gutierrez-Ramos, J. C. (2000) *Immunity* **13,** 95–105
15. Suh, W. K., Tafuri, A., Berg-Brown, N. N., Shahinian, A., Plyte, S., Duncan, G. S., Okada, H., Wakeham, A., Odermatt, B., Ohashi, P. S., and Mak, T. W. (2004) *J. Immunol.* **172,** 5917–5923
16. Dong, C., Juedes, A. E., Temann, U. A., Shresta, S., Allison, J. P., Ruddle, N. H., and Flavell, R. A. (2001) *Nature* **409,** 97–101
17. Dong, C., Temann, U. A., and Flavell, R. A. (2001) *J. Immunol.* **166,** 3659–3662
18. McAdam, A. J., Greenwald, R. J., Levin, M. A., Chernova, T., Malenkovich, N., Ling, V., Freeman, G. J., and Sharpe, A. H. (2001) *Nature* **409,** 102–105
19. Tafuri, A., Shahinian, A., Bladt, F., Yoshinaga, S. K., Jordana, M., Wakeham, A., Boucher, L. M., Bouchard, D., Chan, V. S., Duncan, G., Odermatt, B., Ho, A., Itie, A., Horan, T., Whoriskey, J. S., Pawson, T., Penninger, J. M., Ohashi, P. S., and Mak, T. W. (2001) *Nature* **409,** 105–109
20. Akiba, H., Takeda, K., Kojima, Y., Usui, Y., Harada, N., Yamazaki, T., Ma, J., Tezuka, K., Yagita, H., and Okumura, K. (2005) *J. Immunol.* **175,** 2340–2348
21. Grimbacher, B., Hutloff, A., Schlesier, M., Glocker, E., Warnatz, K., Drager, R., Eibel, H., Fischer, B., Schaffer, A. A., Mages, H. W., Kroczek, R. A., and Peter, H. H. (2003) *Nat. Immunol.* **4,** 261–268
22. Warnatz, K., Bossaller, L., Salzer, U., Skrabl-Baumgartner, A., Schwinger, W., van der, B. M., van Dongen, J. J., Orlowska-Volk, M., Knoth, R., Durandy, A., Draeger, R., Schlesier, M., Peter, H. H., and Grimbacher, B. (2005) *Blood* **107,** 3045–3052
23. Harada, H., Salama, A. D., Sho, M., Izawa, A., Sandner, S. E., Ito, T., Akiba, H., Yagita, H., Sharpe, A. H., Freeman, G. J., and Sayegh, M. H. (2003) *J. Clin. Invest.* **112,** 234–243
24. Rottman, J. B., Smith, T., Tonra, J. R., Ganley, K., Bloom, T., Silva, R.,

Pierce, B., Gutierrez-Ramos, J. C., Ozkaynak, E., and Coyle, A. J. (2001) *Nat. Immunol.* **2,** 605–611
25. Zheng, Y., Jost, M., Gaughan, J. P., Class, R., Coyle, A. J., and Monestier, M. (2005) *J. Immunol.* **174,** 3117–3121
26. Akbari, O., Freeman, G. J., Meyer, E. H., Greenfield, E. A., Chang, T. T., Sharpe, A. H., Berry, G., DeKruyff, R. H., and Umetsu, D. T. (2002) *Nat. Med.* **8,** 1024–1032
27. Coyle, A. J., and Gutierrez-Ramos, J. C. (2004) *Springer Semin. Immunopathol.* **25,** 349–359
28. Ozkaynak, E., Gao, W., Shemmeri, N., Wang, C., Gutierrez-Ramos, J. C., Amaral, J., Qin, S., Rottman, J. B., Coyle, A. J., and Hancock, W. W. (2001) *Nat. Immunol.* **2,** 591–596
29. McAdam, A. J., Chang, T. T., Lumelsky, A. E., Greenfield, E. A., Boussiotis, V. A., Duke-Cohan, J. S., Chernova, T., Malenkovich, N., Jabs, C., Kuchroo, V. K., Ling, V., Collins, M., Sharpe, A. H., and Freeman, G. J. (2000) *J. Immunol.* **165,** 5035–5040
30. Sarafova, S., and Siu, G. (1999) *J. Biol. Chem.* **274,** 16126–16134
31. Casolaro, V., Keane-Myers, A. M., Swendeman, S. L., Steindler, C., Zhong, F., Sheffery, M., Georas, S. N., and Ono, S. J. (2000) *J. Biol. Chem.* **275,** 36605–36611
32. Faltynek, C. R., Schroeder, J., Mauvais, P., Miller, D., Wang, S., Murphy, D., Lehr, R., Kelley, M., Maycock, A., Michne, W., Miski, M., and Thunberg, A. L. (1995) *Biochemistry* **34,** 12404–12410
33. Rudd, C. E., and Schneider, H. (2003) *Nat. Rev. Immunol.* **3,** 544–556
34. Pages, F., Ragueneau, M., Rottapel, R., Truneh, A., Nunes, J., Imbert, J., and Olive, D. (1994) *Nature* **369,** 327–329
35. Prasad, K. V., Cai, Y. C., Raab, M., Duckworth, B., Cantley, L., Shoelson, S. E., and Rudd, C. E. (1994) *Proc. Natl. Acad. Sci. U. S. A.* **91,** 2834–2838
36. Stein, P. H., Fraser, J. D., and Weiss, A. (1994) *Mol. Cell Biol.* **14,** 3392–3402
37. Macian, F. (2005) *Nat. Rev. Immunol* **5,** 472–484
38. Rao, A., Luo, C., and Hogan, P. G. (1997) *Annu. Rev. Immunol.* **15,** 707–747
39. Cannons, J. L., Yu, L. J., Hill, B., Mijares, L. A., Dombroski, D., Nichols, K. E., Antonellis, A., Koretzky, G. A., Gardner, K., and Schwartzberg, P. L. (2004) *Immunity* **21,** 693–706
40. Loots, G. G., and Ovcharenko, I. (2005) *Nucleic Acids Res.* **33,** W56–W64
41. Quandt, K., Frech, K., Karas, H., Wingender, E., and Werner, T. (1995) *Nucleic Acids Res.* **23,** 4878–4884
42. Fruman, D. A., Pai, S. Y., Burakoff, S. J., and Bierer, B. E. (1995) *Mol. Cell Biol.* **15,** 3857–3863
43. Hogan, P. G., Chen, L., Nardone, J., and Rao, A. (2003) *Genes Dev.* **17,** 2205–2232
44. Macian, F., Lopez-Rodriguez, C., and Rao, A. (2001) *Oncogene* **20,** 2476–2489
45. Ling, V., Wu, P. W., Finnerty, H. F., Agostino, M. J., Graham, J. R., Chen, S., Jussiff, J. M., Fisk, G. J., Miller, C. P., and Collins, M. (2001) *Genomics* **78,** 155–168
46. Arimura, Y., Kato, H., Dianzani, U., Okamoto, T., Kamekura, S., Buonfiglio, D., Miyoshi-Akiyama, T., Uchiyama, T., and Yagi, J. (2002) *Int. Immunol.* **14,** 555–566
47. Nurieva, R. I., Duong, J., Kishikawa, H., Dianzani, U., Rojo, J. M., Ho, I., Flavell, R. A., and Dong, C. (2003) *Immunity* **18,** 801–811
48. Wassink, L., Vieira, P. L., Smits, H. H., Kingsbury, G. A., Coyle, A. J., Kapsenberg, M. L., and Wierenga, E. A. (2004) *J. Immunol.* **173,** 1779–1786
49. Shilling, R. A., Pinto, J. M., Decker, D. C., Schneider, D. H., Bandukwala, H. S., Schneider, J. R., Camoretti-Mercado, B., Ober, C., and Sperling, A. I. (2005) *J. Immunol.* **175,** 2061–2065